

$\pi^\pm$  Spectra in Au+Au Collisions at  $\sqrt{s_{NN}}=62.4$  GeVZhangbu Xu<sup>1</sup> for the STAR Collaboration<sup>1</sup>*Physics Department, Brookhaven National Laboratory, Upton, NY 11973, USA*

The combination of the ionization energy loss ( $dE/dx$ ) from Time Projection Chamber (TPC) at  $\simeq 8\%$  resolution and multi-gap resistive plate chamber time-of-flight (TOF) at  $85ps$  provides powerful particle identification. We present spectra of identified charged pions from transverse momentum  $p_T \simeq 0.2$  GeV/c to  $7-8$  GeV/c in Au+Au collisions at  $\sqrt{s_{NN}} = 62.4$  GeV. Physics implications will be discussed.

*Keywords:*  $dE/dx$ ; particle identification; jet quenching; nuclear modification factor

In this report, we studied charged  $\pi^\pm$  spectra and their nuclear modification factors in Au+Au collisions at  $\sqrt{s_{NN}}=62.4$  GeV. Identification of  $\pi^\pm$  was made possible by ionization energy loss ( $dE/dx$ ) of charged particle traversing Time Projection Chamber (TPC)<sup>1</sup>, and time-of-flight (TOF) from a prototype multi-gap resistive plate chamber<sup>2</sup>. The relativistic rise of  $dE/dx$  ( $\mathbf{rdE/dx}$ ) in TPC alone can identify  $\pi^\pm$  from  $3 \lesssim p_T \lesssim 10$  GeV/c. TOF extends the identification to lower  $p_T$ , and help confirm the  $dE/dx$  calibration.

Ionization energy loss of charged particles traversing TPC has been used to identify hadrons at low momentum in STAR for identified particle spectra, flow, and HBT studies. The relativistic rise of  $dE/dx$  also separates the electrons from the hadrons. With additional hadron rejection capability from TOF, we were able to develop a hadron-blind detector<sup>3</sup> for lepton identification at low  $p_T$ . The measurement of  $dE/dx$  is a truncated-mean method in which 30% at the high tail of  $dE/dx$  samples in a track are discarded<sup>1</sup>. The  $dE/dx$  resolution has been found to be between 6% and 11%, depending on the magnetic field setting, event multiplicity, beam luminosity, track length and drift distance. It was calibrated to be better than 8% in Au+Au collisions at  $\sqrt{s_{NN}}=62.4$  GeV for tracks with 70 cm in length. At momentum  $p \gtrsim 3$  GeV/c, the  $dE/dx$  of  $\pi^\pm$  has a  $\sim 15\%$  ( $\sim 2\sigma$ ) separation from that of  $K^\pm$  and  $p(\bar{p})$  due to the relativistic rise of pion  $dE/dx$  at large  $\beta\gamma$ . This allows us to identify charged pions at  $3 \lesssim p_T \lesssim 10$  GeV/c.

The  $dE/dx$  measurement presented in Fig. 1 uses a normalized  $dE/dx$ :  $n\sigma_X^Y = \ln((dE/dx)^Y / I_{0,X}) / \sigma_X$  where  $X, Y$  can be  $e^\pm, \pi^\pm, K^\pm$  or  $p(\bar{p})$ , and  $I_{X0}$  is the expected  $dE/dx$  of particle  $X$ . With perfect calibration, the  $n\sigma_\pi^\pi$  distribution will be a normal Gaussian distribution, and  $n\sigma_\pi^p$  at high  $p_T$  will be a Gaussian peaking at negative value due to smaller  $dE/dx$  of proton traversing TPC. Fig. 2 shows  $p_T$  dependence of  $n\sigma_\pi^K$  and  $n\sigma_\pi^p$  as predicted by Bichsel Functions for the energy loss in thin layers of argon<sup>1</sup>. As shown in Fig. 1 and measurements from TOF<sup>4</sup>,  $(h^+ - h^-) = (p - \bar{p}) + (K^+ - K^-) + (\pi^+ - \pi^-) \simeq p - \bar{p}$ . Therefore, the peak positions

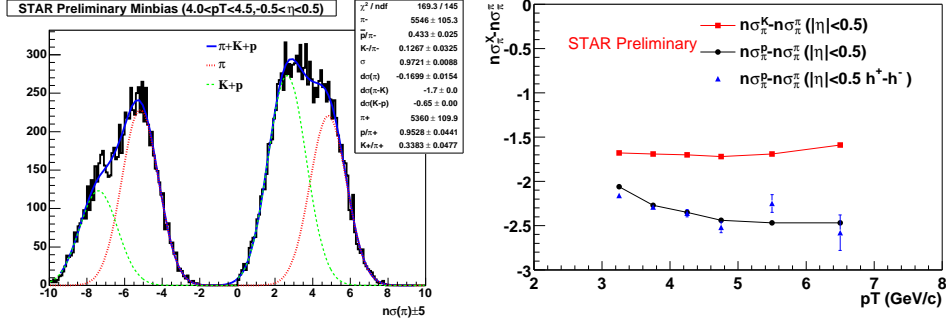


Fig. 1.  $dE/dx$  distribution normalized by pion  $dE/dx$  and offset by  $\pm 5$  for positive and negative  $\pi$  (squares) and  $p-\pi$  (circles) in unit of standard charge at  $4 < p_T < 4.5$  GeV/c, respectively. The distribution is from minimum-bias Au+Au collisions. The triangles are the peak positions of the  $dE/dx$  distribution of  $(h^+ - h^-)$ .

of  $dE/dx$  distribution from  $(h^+ - h^-)$  should represent well that of proton. Indeed, the calibrated Bichsel Function for proton matches well with the  $dE/dx$  peak position of  $(h^+ - h^-)$ . In addition, the  $dE/dx$  difference of protons and pions in the momentum region where PID selection is possible by TOF has been checked to be consistent with Bichsel Function. These give us confidence that Bichsel Function can be used to constrain the relative  $dE/dx$  position between kaons, protons and pions. In the following analysis, we fixed  $n\sigma_\pi^K - n\sigma_\pi^\pi$  and  $n\sigma_\pi^p - n\sigma_\pi^\pi$  in a six Gaussian fit, where the six Gaussians are for  $\pi^\pm$ ,  $K^\pm$  and  $p(\bar{p})$  at a given  $p_T$  bin.

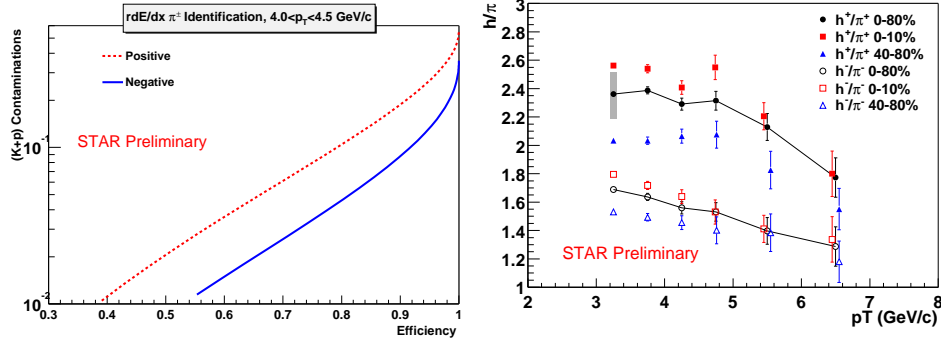


Fig. 3. Contamination from K+p to pions with a  $dE/dx$  selection window vs pion efficiency from the same selection. Dashed line is for  $\pi^+$  and solid line is from  $\pi^-$ .

Although a fit procedure was used to extract the particle yields, pion identification can be done track by track instead of statistically. Fig 3 illustrates the contamination from kaons and protons to pions when we select  $n\sigma_\pi$  greater than a

Fig. 4.  $h^\pm/\pi^\pm$  ratios vs  $p_T$  for three centralities. We varied  $n\sigma_\pi^{K,p}$  around Bichsel Function to estimate the systematical uncertainty which is highly correlated among centralities.

given value. We can achieve  $> 95\%$  pion purity at 50% pion efficiency with a cut of  $n\sigma_\pi > 0$ . As shown in Fig. 2, the separation of dE/dx of protons from kaons is close to  $1\sigma$  at high momentum, studies are underway to reliably identify protons. These open doors to identified particle jet spectra, correlation, anisotropic flow at high  $p_T$  with high statistics.

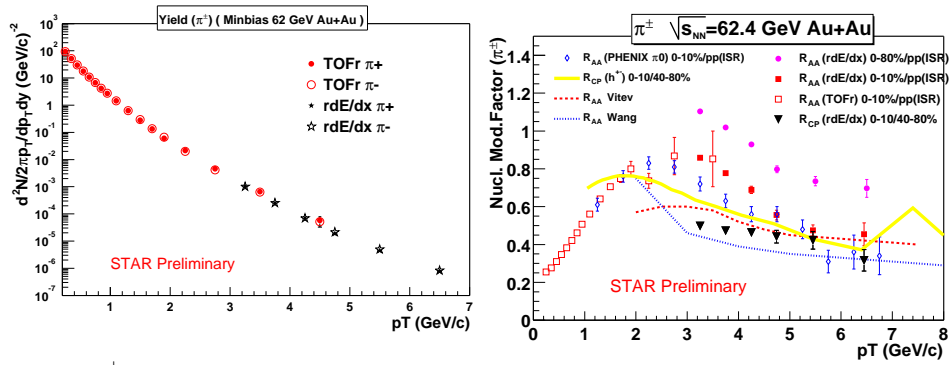


Fig. 5.  $\pi^\pm$  spectra in minimum-bias Au+Au collisions from TOF and TPC rdE/dx.  $\pi^+/\pi^- \simeq 1$  while  $(h^+/h^-)$  is much larger than unity.

Fig. 6. Nuclear modification factors ( $R_{AA}$  and  $R_{CP}$ ) for  $\pi^\pm,0$  and inclusive hadrons. Reference spectrum of p+p is from ISR <sup>5</sup>.

Since  $\pi^\pm$  and inclusive hadrons ( $h^\pm$ ) can be identified in the same detector with only small dE/dx difference, we can obtain  $h^\pm/\pi^\pm$  with high precision. Fig. 4 shows  $h^\pm/\pi^\pm$  ratios vs  $p_T$  for three centralities. The  $h^\pm/\pi^\pm$  in central collisions approach those in peripheral collisions at  $p_T \gtrsim 5$  GeV/c, indicating an absence of particle type dependence of nuclear effect at high  $p_T$ . Difference of particle composition between negative and positive hadrons is evident. Fig. 5 shows  $\pi^\pm$  spectra in minimum-bias Au+Au collisions from TOF <sup>4</sup> and TPC rdE/dx. The two spectra agree well within statistical uncertainty. Fig. 6 shows nuclear modification factors of charged pions, and the comparisons to those of  $\pi^0$  <sup>5</sup>, inclusive hadrons <sup>6</sup> and theoretical predictions <sup>7,8</sup>. At  $p_T \gtrsim 5$  GeV/c,  $R_{AA}$  and  $R_{CP}$  approach each other and agree with the predictions. At lower  $p_T$ ,  $R_{AA}$ ,  $R_{CP}$  and the predictions diverge.

## References

1. M. Anderson *et al.*, *Nucl. Instr. Meth. A* **499** (2003) 659.
2. J. Adams *et al.*(STAR), Arxiv: nucl-ex/0309012.
3. J. Adams *et al.*(STAR), Arxiv: nucl-ex/0407006; L.J. Ruan, *et al.*, nucl-ex/0403054.
4. M. Shao *et al.*(STAR), Hot Quarks 2004, July 18-24, 2004, Taos Valley, New Mexico.
5. D. d'Enterria *et al.*(PHENIX), Hot Quarks 2004.
6. J. Dunlop *et al.*(STAR), RHIC & AGS Annual Users Meeting, May 10-14, 2004.
7. I. Vitev, Arxiv: nucl-th/0404052, Curve shown is calculation with  $dN_g/dy = 650$ .
8. X.N. Wang, *Phys. Rev. C* **70** (2004) 031901.